Targeting metabolic reprogramming promotes the efficacy of transarterial chemoembolization in the rabbit VX2 liver tumor model

YI LUO[1], YONG YANG[2], MEIZE YE[3] and JING ZUO[2]

[1]Department of Interventional Radiology; [2]Department of Oncology, The Second Hospital of Wuhan Iron and Steel (Group) Corp., Wuhan, Hubei 430022; [3]Department of Interventional Radiology, Huazhong University of Science and Technology, Wuhan, Hubei 430000, P.R. China

Received July 25, 2023; Accepted November 30, 2023

DOI: 10.3892/ol.2024.14244

Abstract. Transarterial chemoembolization (TACE) may prolong the survival of patients with hepatocellular carcinoma (HCC); however, its efficacy is limited due to the high rate of incomplete embolization. Hypoxia after embolization can cause a series of changes in the tumor microenvironment, including lactate dehydrogenase A (LDHA) upregulation. Therefore, the current study assessed the antitumor effect and the underlying mechanism of the LDHA inhibitor, sodium oxamate (Ox), combined with TACE, using the rabbit VX2 liver tumor model. VX2 liver tumor models were created in the left liver lobe of rabbits, and after 14 days of treatments, the rabbits were sacrificed for the collection of the tumor tissues and blood samples. The antitumor effects of Ox, and the combination of Ox and TACE, and changes in the tumor microenvironment after treatments were assessed by histopathological evaluation, and the safety of the treatments was analyzed by measuring changes in the serum levels of alanine aminotransferase, aspartate aminotransferase, blood urea nitrogen and creatinine. The results demonstrated that the combination of Ox and TACE notably improved antitumor effects compared with in the other groups, as it significantly inhibited tumor growth. Additionally, treatment with Ox + TACE downregulated vascular endothelial growth factor and matrix metalloproteinase-9, and enhanced the infiltration of $CD3^+$ and $CD8^+$ T cells into tumor tissues, thus suggesting that Ox + TACE may have a synergistic effect on increasing the infiltration of immune cells in the tumor microenvironment. With a well-tolerated and manageable impairment of hepatorenal function, targeting metabolic reprogramming could promote the efficacy of TACE, thus providing novel avenues for the future clinical management of patients with advanced HCC.

Correspondence to: Dr Jing Zuo, Department of Oncology, The Second Hospital of Wuhan Iron and Steel (Group) Corp., 400 Qinghua Road, Qingshan, Wuhan, Hubei 430022, P.R. China
E-mail: lilaczj@126.com

Key words: metabolic reprogramming, transarterial chemoembolization, sodium oxamate, antitumor immune response

Introduction

Hepatocellular carcinoma (HCC) is the second leading cause of cancer-related mortality worldwide and the most common pathological subtype of liver cancer (1,2). The prognosis of HCC remains unsatisfactory, with a 5-year survival rate of ~18% (3). A previous study suggested that transarterial chemoembolization (TACE) can control intermediate-stage HCC and improve the 5-year survival rate of patients (4). Therefore, TACE has been recommended by several authorities as a first-line therapy for treating patients with HCC (5). However, due to the high rate of incomplete embolization, TACE remains inadequate in controlling HCC growth as a palliative treatment approach (6).

Several studies on tumor metabolism have highlighted the association between energy availability and cell proliferation, and the critical role of metabolic reprogramming in neoplastic cells (7). Metabolism is abnormal in solid tumors and is characterized by a higher glycolytic rate and glucose absorption, thus promoting the production of high concentrations of lactate; this process is widely known as the Warburg effect or aerobic glycolysis (8). Unlike normal cells, neoplastic cells display an enhanced metabolism to maintain a reduction-oxidation balance and provide enough energy for cancer cell proliferation and growth (9). The aforementioned features have been reported in several types of solid tumors, including HCC, colon cancer and breast cancer (10,11).

Lactate dehydrogenase A (LDHA) is a key enzyme in the aerobic glycolytic pathway, as it converts lactate to pyruvate (12). During the Warburg effect, ATP generation is more rapid in cancer cells compared with that in normal cells (13). In addition, a study reported that cancer cells can secrete lactate into the extracellular matrix, thus enhancing cell motility, invasion and metastasis via upregulating metalloproteases (14). Moreover, lactate has been reported to decrease the activation and differentiation of dendritic cells (15), and inhibit tumor surveillance via T and natural killer cells (16). It has also

been reported that hypoxia-inducible factor-1α (HIF-1α), as a key factor in hypoxic adaptation, can activate the expression of glycolytic enzymes, including LDHA (17). Another study demonstrated that TACE can upregulate HIF-1α due to the high rate of incomplete embolization, thus further increasing the expression of LDHA in residual tumors (18). Furthermore, LDHA overexpression has been reported to be associated with tumor development, particularly in disseminated types of cancer, including hypoxic carcinoma and metastatic cancer cells, thus leading to a poor prognosis (19). Additionally, a previous study indicated that LDHA inhibition can suppress tumor growth (20). Therefore, targeting metabolic reprogramming to directly inhibit glycolysis and ATP generation could be a feasible protocol for patients with HCC treated with TACE.

Sodium oxamate (Ox) is an analog of pyruvate, which acts as a competitive inhibitor. Emerging evidence has demonstrated that Ox can inhibit LDHA and the Warburg effect (21-23). Therefore, the current study assessed the therapeutic efficacy of a combination of Ox and TACE in a rabbit VX2 liver tumor model via the evaluation of tumor growth. To assess the mechanism underlying the antitumor effect of Ox + TACE therapy, immune responses, cell metastasis and angiogenesis were evaluated in the tumor microenvironment by immunohistochemical analysis. In addition, to assess the biocompatibility of the combination therapy, changes in hepatorenal function were measured.

Materials and methods

Materials. Ox (cat. no. sc-215880) was purchased from Santa Cruz Biotechnology, Inc., whilst iohexol (Omnipaque™), ethiodized oil (Lipiodol®) and polyvinyl alcohol (PVA) foam embolization particles (Ivalon®; 180-300 mm) were purchased from Guerbet Laboratories Ltd., B. Braun Melsungen AG and Cook Medical, respectively. All reagents were of chemical pure or analytical grade, and were used as purchased without any further purification.

New Zealand white rabbits (n=48; weight, 2.5-3 kg; 24 male and 24 female rabbits; age, 10-12 weeks) were obtained from Liaoning Changsheng Biotechnology Co., Ltd. All animal experiments were carried out according to the Chinese National Animal Law on the use of laboratory animals. All animal welfare considerations were taken, including efforts to minimize suffering and distress, use of analgesics or anaesthetics and special housing conditions [20˚C; ventilation rate, 2-3 m^3/h; 14/10-h light/dark cycle; humidity, 60-65%; pellet feed, 150 g/day, twice a day; automatic water supply system (free access)]. All rabbits were euthanized by intraperitoneal injection of 100 mg/kg pentobarbital sodium. At 20 min after the injection, death was confirmed by checking respiration, heartbeat, pupil and nerve reflex. All procedures were approved by the Animal Care and Use Committee of Huazhong University of Science and Technology (Wuhan, China; 2023; approval no. 3380).

Establishment of the rabbit VX2 liver tumor model. All interventional procedures were performed by a radiologist with ≥15 years of experience. The rabbit VX2 liver tumor model was established as previously described (24). A 12-week-old tumor-bearing male rabbit was purchased from the Animal Center of Huazhong University of Science and Technology; the VX2 tumor was collected at 14 days since xenograft implantation, and the tumor was collected after the rabbit was sacrificed by intraperitoneal injection of 100 mg/kg pentobarbital sodium. At 20 min after the injection, death was confirmed by checking respiration, heartbeat, pupil and nerve reflex. Then, the VX2 tumor was sliced into 1.0 mm^3 pieces and, under gas anesthesia (3-4% isoflurane used for induction and 2% for maintenance), a piece of the VX2 tissue was implanted into the left liver lobe of the rabbits (24). To avoid infection, the wounds were topically treated with $2.0x10^4$ IU gentamycin, while rabbits were also administered an intramuscular injection of $1.0x10^4$ IU ampicillin (25). No adverse effects were observed after injection of ampicillin.

A total of 24 VX2-tumor-bearing rabbits were randomly divided into the following four groups (n=6 rabbits/group; treatment duration, 14 days): Control group, normal saline was injected into the tumor-feeding arteries (control group); TACE group, TACE was performed via delivering a mixture of 0.3 ml Lipiodol mixed with 6 mg doxorubicin into the tumor-feeding arteries. The arteries were then occluded with PVA foam embolization particles; Ox group Ox, the tumor-feeding arteries were injected with an intra-arterial bolus of Ox saline (5 mg/kg; 5 min); and TACE + Ox group, the tumor-feeding arteries were injected with an intra-arterial bolus of Ox saline (5 mg/kg; 5 min), followed by TACE. When the VX2 tumor volume reached 1.61 cm^3, TACE was performed in the TACE and TACE + Ox groups using a 2.7F microcatheter (Terumo Corporation), guided by digital subtraction angiography (Siemens Healthineers). The tumor-feeding arteries were continuously monitored during TACE until the tumor blood supply was completely occluded (no delivery of contrast agent was visible in tumoral and peritumoral vessels), with the normal hepatic artery unobstructed; the contrast agent used for angiography was Iohexol.

Tumor growth and rabbit survival follow-up. A 320-row spiral computed tomography (CT; Siemens Healthineers) was used for plain scan and contrast-enhanced CT. The contrast-enhanced CT was performed to assess the therapeutic effects of different treatments at 14 days. CT was repeated at days 3, 7, 10 and 14 to record the metastasis in the four groups. Tumor volume was calculated using CT (80 kV; 100 mA; 1-mm slice thickness; 1.1 pitch; 200x200-mm^2 field of view) with the following formula: $V=a \times b \times c \times \pi/6$, where a, b and c indicate the anteroposterior, transverse and axial diameters, respectively. In addition, the survival of all treated rabbits (an additional 6 rabbits/group) was recorded. Animal health and behaviour were monitored every day and the rabbits were euthanized when the tumor weight reached ≤10% of their weight or when pain could not be effectively controlled during observation. The rabbits were considered to be in pain when they were abnormally vocal, or when they licked, bit, scratched or shook the painful area. The time of euthanasia or death was recorded, which was used to indicate mortality.

Sample collection. Blood samples were collected from the auricular vein of the rabbits under anesthesia (3-4% isoflurane used for induction and 2% for maintenance) in each treatment

group (2 ml/collection; once daily on days 0, 1, 3, 7 and 14). The 14-day blood samples were collected before euthanasia. Subsequently, the samples were centrifuged (4˚C, 1,000 x g, 10 min) to obtain serum, which was then stored at -80˚C until use. The tumor and peritumoral tissues from each group were fixed in 4% formalin overnight at 25˚C and paraffin-embedded at 52-54˚C. The paraffin-embedded tissues were then cut into 5.0-μm slices for histological analysis.

Biochemical analyses. To measure the levels of biochemical markers in serum *in vivo*, the blood samples from all four groups were collected and centrifuged at 1,000 x g for 10 min at 4˚C to collect serum. The levels of the biochemical markers alanine aminotransferase (ALT), aspartate aminotransferase (AST), blood urea nitrogen (BUN) and creatinine (CRE) in serum were measured using a biochemical auto-analyzer (Model DXC8000; Beckman Coulter, Inc.).

Histological analysis. For rehydration, tissue sections were immersed in a descending ethanol series. Subsequently, antigen retrieval in 1 mM EDTA (pH 8.0) was performed at 98˚C for 15 min followed by washing twice in PBS and distilled water. For permeabilization, the Permeabilization Wash Buffer (cat. no. 40403ES64; Shanghai Yeasen Biotechnology Co., Ltd.) was used, after which, tissues were blocked in 10% normal goat serum (cat. no. C0265; Beyotime Institute of Biotechnology) for 20 min at 25˚C. H_2O_2 (3%, 50 μl) was used to block endogenous peroxidase. The tissue sections were then incubated with anti-matrix metalloproteinase-9 (MMP-9; 1:1,000; cat. no. GB12132-100; Wuhan Servicebio Technology Co., Ltd.), anti-CD3 (1:100; cat. no. GB12014-100; Wuhan Servicebio Technology Co., Ltd.), anti-CD8 (1:100; cat. no. GB12068-100; Wuhan Servicebio Technology Co., Ltd.) and anti-vascular endothelial growth factor (VEGF; 1:150; cat. no. AB1876-I; MilliporeSigma) primary antibodies at 4˚C overnight. Subsequently, the sections were incubated with an anti-mouse HRP (IgG H&L) secondary antibody (cat. no. ab97040; Abcam; 1:1,000) at 37˚C for 1 h. DAB was used for chromogen detection. Tumor tissues also underwent hematoxylin and eosing (H&E) staining, as follows: Sections were stained with hematoxylin at 25˚C for 15 min and eosin at 25˚C for 5 min. In addition, the tumor necrosis ratio (TNR) was calculated using the following formula: TNR=N/(N + T), where N indicates the necrotic areas of the tumor and T indicates the living tumor areas of the tumor (detected by H&E assay). A total of six sections per tumor tissue were observed and the integrated optical density (IOD) sum in five randomly selected fields (magnification, x400; light microscope) was calculated using ImageJ version 22 (National Institutes of Health). The mean values from the five randomly selected fields were calculated and used for statistical analysis.

Immunofluorescence assay. Cell apoptosis was assessed using a Terminal Deoxynucleotidyl Transferase mediated dUTP Nick-End Labeling (TUNEL) assay (cat. no. 12156792910; MilliporeSigma) according to the manufacturer's instructions. In addition, a Ki67 assay (dilution, 1:200; Wuhan Servicebio Technology Co., Ltd.) was used to evaluate tumor cell proliferation according to the manufacturer's instructions. Tumor cell nuclei were stained with DAPI at 25˚C for 20 min. In both fluorescence assays, images were captured by excitation at 488 nm and emission at 560 nm (BX53; Olympus Corporation). A total of six sections were assessed per tumor sample. The IOD sum of the images was calculated using ImageJ. The mean results from five randomly selected fields were calculated and statistical analysis was performed.

Statistical analysis. All statistical analyses were performed using SPSS v24.0 (IBM Corp.) and GraphPad Prism (version 8.0; Dotmatics) software. All data are expressed as the mean ± standard deviation. Kaplan-Meier analysis was used to plot the overall survival curves, and the significance was calculated using the log-rank test. Comparisons among multiple groups were performed using one-way ANOVA, followed by Tukey's Honest Significant Difference test to assess the differences between groups. $P<0.05$ was considered to indicate a statistically significant difference.

Results

Successful operations and establishment of the rabbit VX2 liver tumor model. The liver tumor masses were clearly visible on CT images (Fig. 1A). Prior to treatment, tumor volumes were 1,628.5±20.3, 1,601.8±22.3, 1,608.9±29.8 and 1,630.2±19.2 mm^3 in the control, TACE, Ox and TACE + Ox groups, respectively. No statistically significant difference in tumor volume was demonstrated among the different groups. The TACE procedure is shown in Fig. 1B and C. No rabbits were euthanized or found dead before the end of the experiment and all tumor tissues and serum samples were successfully collected.

Tumor response and survival of treated rabbits. A representative CT image from each treatment group at 14 days after the operation is shown in Fig. 2A. Tumor growth rate was notably reduced in the TACE (202.7±46.23%) and Ox (203.0±54.47%) groups, and significantly reduced in the TACE + Ox (96.8±20.31%) group compared with that of the control group (248.2±45.50%; Fig. 2B). Rabbits in the TACE + Ox group demonstrated a significantly improved tumor response compared with those in the TACE ($P<0.001$) and Ox ($P<0.001$) groups. No statistically significant difference was observed between the TACE and Ox groups ($P>0.999$; Fig. 2B). Representative tumor tissues of each group after treatment for 14 days are presented in Fig. 2C. The majority (94.7%) of tumor tissues in the TACE + Ox group were necrotic. Furthermore, compared with in the control group (28.12±8.91%), TNR was significantly enhanced in the TACE (60.25±12.25%; $P<0.001$), Ox (62.23±9.32%; $P<0.001$) and TACE + Ox (90.62±4.96%; $P<0.001$) groups. Notably, the combination demonstrated a significantly better TNR than that of the Ox group; the combination group demonstrated the greatest TNR (Fig. 2D and E). Subsequently, to assess the survival benefits of TACE, Ox and TACE + Ox therapy in VX2-bearing rabbits, the ability of the different treatments to promote survival was compared. Significant survival benefits were observed in rabbits in the combination group compared with those in the control ($P<0.001$), TACE ($P<0.001$) and Ox ($P<0.001$) groups (Fig. 2F). The number of metastases during follow-up is demonstrated in Fig. 2G. The metastases occurred at day

Figure 1. (A) Tumor shown using computed tomography prior to the operation. Arterial angiography of the VX2 liver tumor in the rabbits (B) prior to and (C) immediately after transarterial chemoembolization, in which tumor staining disappeared after embolization. The red circle indicates the location of the tumor.

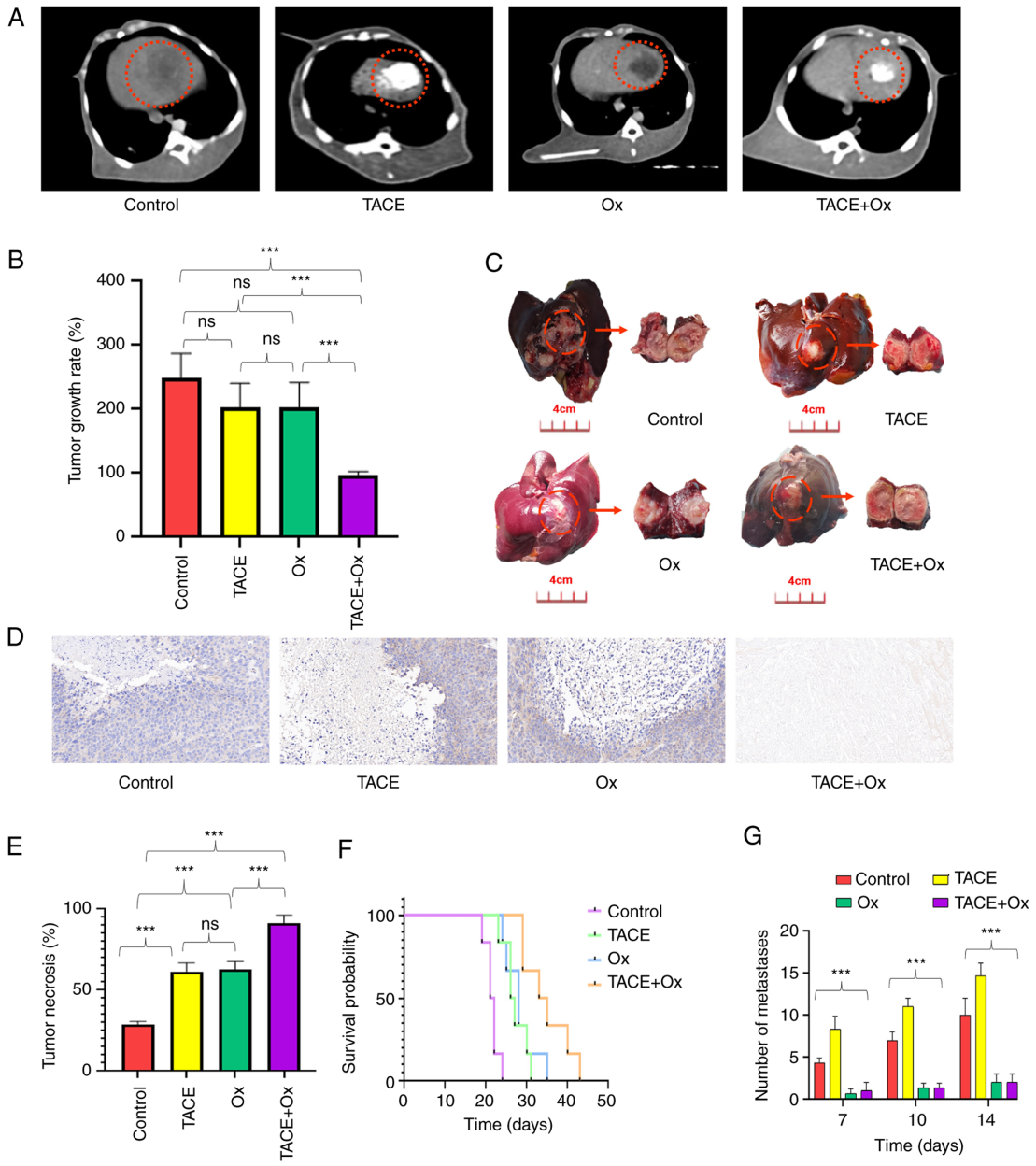

Figure 2. (A) Representative computed tomography images of the four groups after 14 days of treatment. (B) Tumor growth rates in each group of rabbits after therapy. (C) Representative images of liver tumor tissue in each treatment group. (D) Hematoxylin and eosin staining of tumor necrosis in the four groups. (E) Quantitative analysis of the proportion of tumor necrosis, (F) survival rates and (G) number of metastases in each treatment group. ***P<0.001. TACE, transarterial chemoembolization; Ox, sodium oxamate; ns, not significant.

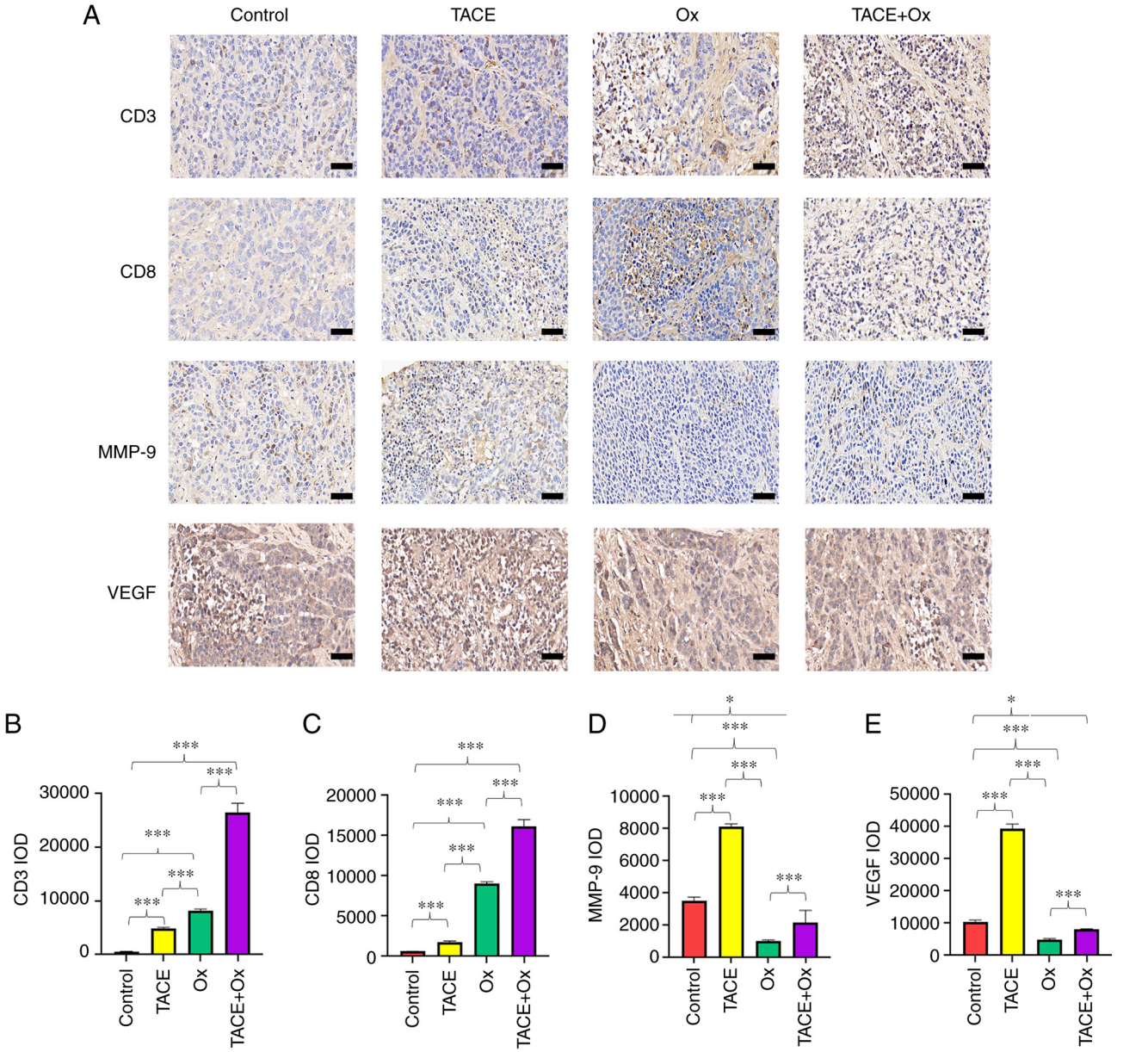

Figure 3. (A) Immunohistochemical staining was performed to determine the number of $CD3^+$ and $CD8^+$ T-lymphocytes, and the protein expression levels of MMP-9 and VEGF in VX2 tumor-bearing rabbits at 14 days after treatment. Scale bar, 100 μm. Semi-quantitative analysis of (B) $CD3^+$, (C) $CD8^+$, (D) MMP-9^+ and (E) $VEGF^+$ cells. $^*P<0.05$; $^{***}P<0.001$. TACE, transarterial chemoembolization; Ox, sodium oxamate; MMP-9, matrix metalloproteinase-9; VEGF, vascular endothelial growth factor; IOD, integrated optical density.

7 and gradually increased in the control and TACE groups. Conversely, Ox exhibited an inhibition of metastasis. The volume of metastasized tumors was 263.7±44.4, 342.1±32.2, 52.1±23.8 and 51.6±18.9 mm^3 in the control, TACE, Ox and TACE + Ox groups after 14 days of treatments ($P<0.001$), repectively.

Changes in tumor microenvironment after treatment. Semi-quantitative analysis of IHC staining revealed that the administration of Ox significantly enhanced the infiltration of $CD3^+$ and $CD8^+$ cells in tumor tissues compared with that in the control group. Although TACE alone also significantly increased the infiltration of the aforementioned cells compared with that in the control group, its capacity was notably attenuated compared with the Ox and TACE + Ox groups (Fig. 3A-C). In addition, although the application of TACE significantaly upregulated MMP-9 in the tumor tissues, treatment with Ox significantly decreased the expression of MMP-9 in the combination group compared with that in the control group (Fig. 3A and D). Moreover, the results indicated that Ox significantly decreased the expression of VEGF compared with that in the control group, and VEGF expression was significantly reduced in the TACE + Ox group compared with that in the control group (Fig. 3A and E). Furthermore, the immunofluorescence staining results demonstrated that the protein expression of Ki67 was significantly decreased in tumors in the TACE + Ox group compared with that in the control, TACE and Ox groups (Fig. 4A and C). Finally, the number of $TUNEL^+$ cells was markedly increased in the TACE + Ox group compared with that in the other groups (Fig. 4A and D).

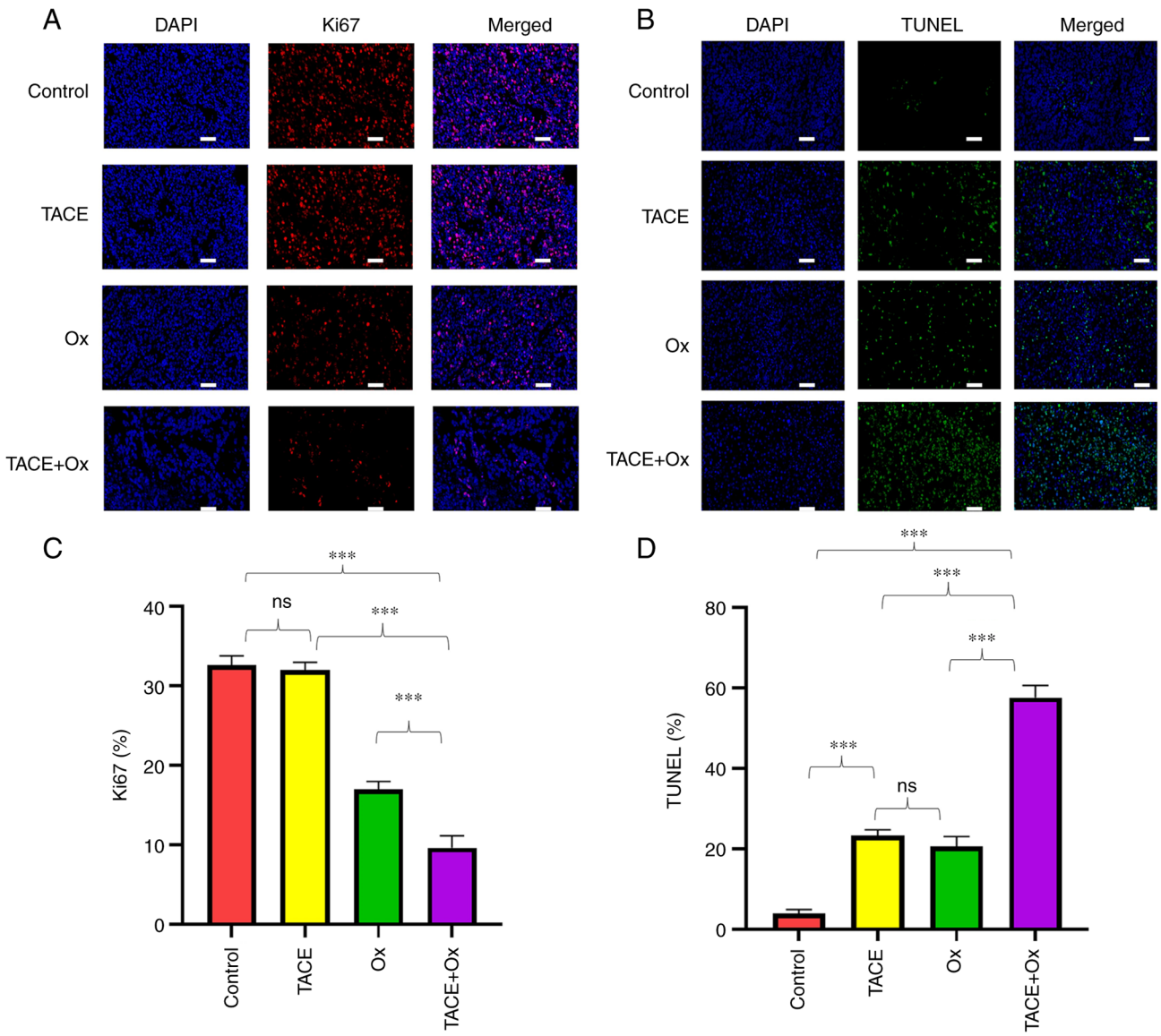

Figure 4. (A) Tumor cell proliferation was assessed using Ki67 staining. Scale bar, 100 μm. (B) Tumor cell apoptosis was determined via TUNEL staining. Scale bar, 100 μm. Semi-quantitative analysis of the percentage of (C) Ki67$^+$ and (D) TUNEL$^+$ cells. ***P<0.001. TACE, transarterial chemoembolization; Ox, sodium oxamate; ns, not significant.

Changes of hepatorenal function. The changes in hepatorenal function are demonstrated in Fig. 5. Except from in the control group, rabbits in the TACE and combination groups had transient liver function impairment; the levels of AST and ALT were significantly higher than control on days 1, 3 and 7, and they then returned to normal levels at day 14 (Fig. 5A and B). However, kidney function was only slightly affected (Fig. 5C and D). The levels of ALT, AST, BUN and CRE reached their peaks on day 1 after treatment and gradually recovered (Fig. 5). These findings indicated that combination therapy may cause a transient impairment in hepatorenal function.

Discussion

It has been reported that the efficacy of TACE is associated with local ischemic necrosis caused by embolic material and the anticancer effects mediated by chemotherapy (26). However, hypoxia caused by incomplete TACE may cause LDHA upregulation in tumors, which is the key enzyme in aerobic glycolysis (27). Furthermore, the enhancement of aerobic glycolysis in tumor tissues may promote tumor growth due to the following reasons: i) Enhanced anaerobic glycolysis may counteract the sharp oxygen fluctuation, which could be fatal for cells that rely on oxygen or anaerobic glycolysis for ATP production (28); ii) lactic acid generated via the anaerobic glycolytic pathway could promote the invasion of tumor cells via the upregulation of the monocarboxylate transporter (MCT)1 and MCT2 (29); and iii) tumor cells could simultaneously activate the pentose phosphate pathway to satisfy their anabolic demands and combat oxidative stress (30,31). Therefore, targeting metabolic reprogramming after TACE may be key for the inhibition of tumor growth, thus improving the therapeutic effect of TACE.

In the present study, the improvement of the antitumor effect of TACE combined with the LDHA inhibitor, Ox, and its underlying mechanism were assessed. Firstly, the results demonstrated that the combination therapy enhanced the infiltration of

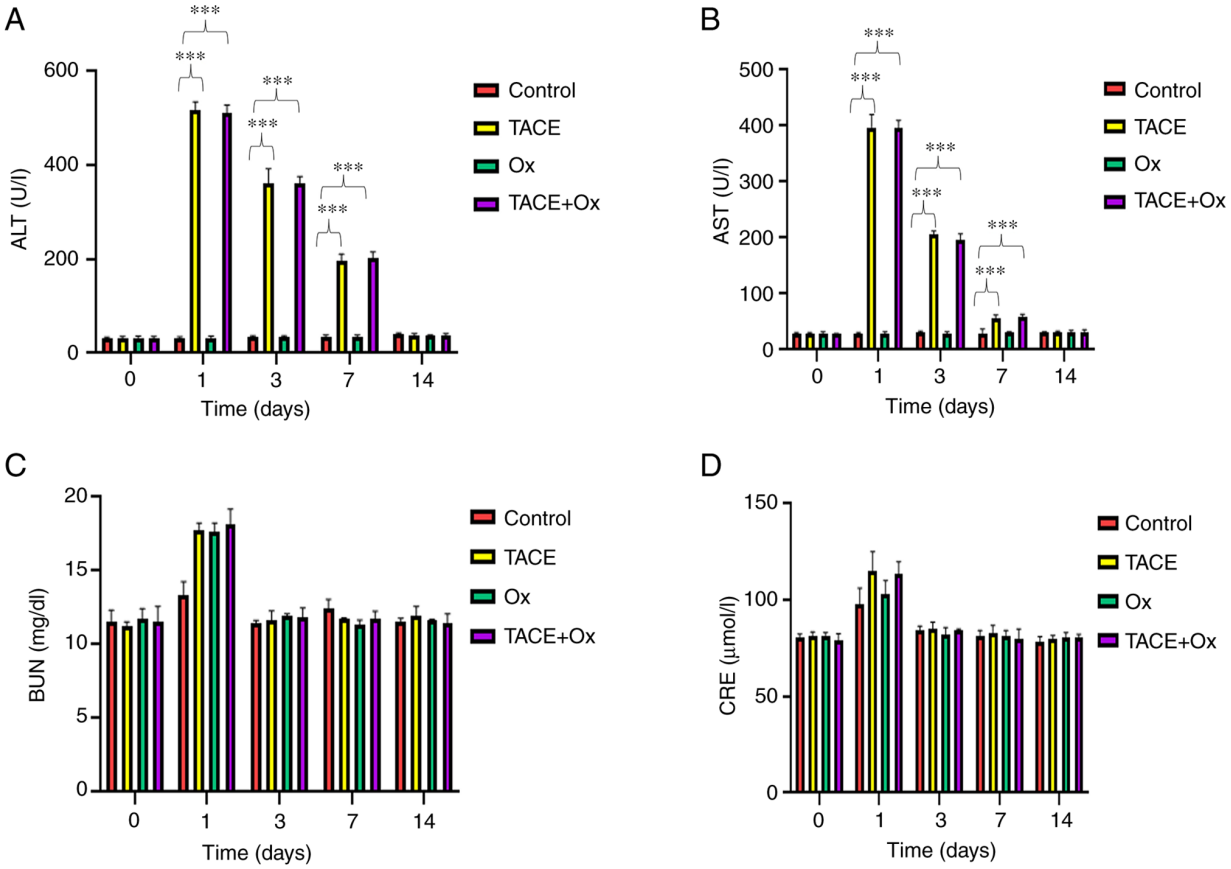

Figure 5. Serum levels of (A) ALT, (B) AST, (C) BUN and (D) CRE, measured at 0, 1, 3, 7 and 14 days after treatment. ***P<0.001. ALT, alanine aminotransferase; AST, aspartate aminotransferase; BUN, blood urea nitrogen; CRE, creatinine; TACE, transarterial chemoembolization; Ox, sodium oxamate.

$CD8^+$ cells. The increase in hypoxic necrosis may be associated with the significantly greater infiltration rate of $CD8^+$ T cells, which is consistent with previous reports (32,33). The findings from a previous study may indicate why Ox increased the infiltration of $CD8^+$ T cells. This previous study indicated that a decrease in lactic acid may downregulate the expression of programmed death-ligand 1, leading to an elevation of pro-inflammatory antitumor responses, such as increased infiltration and activity of $CD8^+$ cytotoxic cells (34). Another study reported that targeting lactic acid metabolism can reduce the production of the angiogenic factor VEGF by downregulating HIF-1α, which contributes to the normalization of tumor blood vessels, and thus increases the infiltration of $CD8^+$ T cells (35). The specific reason for this is worth exploring in-depth in future studies. Furthermore, a previous study reported that the efficacy of immunotherapy was positively associated with the $CD8^+$ T cell to tumor burden ratio (36). Therefore, TACE combined with immunotherapy may be considered as a novel treatment strategy. In the present study, Ox administration downregulated MMP-9; notably, MMP-9 can degrade extracellular matrix components and serves a significant role in several pathophysiological processes, including metastasis, invasion and migration (37). Previous studies have reported that MMP-9 overexpression and dysregulation are associated with the onset of several diseases (38,39). The aforementioned finding may be associated with the reduced lactic acid levels reported in a previous study (40). Furthermore, the administration of Ox could also downregulate VEGF after embolization, which serves a significant role in angiogenesis and tumor cell immune escape (41,42). Lastly, the results of the present study demonstrated that Ox inhibited cell proliferation and promoted apoptosis, which may be associated with a decrease in energy supply to tumor cells and in lactic acid production. The aforementioned mechanisms could result in an improved regulation of the local tumor and increased survival of patients with HCC.

In the present study, although the tumor grew by 202.7±46.23% in the TACE group, the necrosis rate and survival benefits were still greater than that of the control, which is also consistent with the treatment of human liver cancer (43). Moreover, group C (Ox) and B (TACE) demonstrated similar therapeutic results. However, the therapeutic effect in group D was not simply the additive effect of both components. The results demonstrated that the increase in $CD8^+$ T cells and $TUNEL^+$ cells was more than the sum of the other two groups, which may indicate that the protocol had a synergistic therapeutic effect.

In terms of safety, the impairment of hepatorenal function reached its peak at day 1 after treatment and then gradually reduced to normal levels, mimicking TACE. Moreover, Ox monotherapy demonstrated a similar effect to TACE alone without damage to hepatorenal function, indicating that targeting metabolism may be beneficial for patients with HCC. Overall, the results suggested that the combination of Ox and TACE was safe and may only lead to transient and reversable injuries.

However, the present study has certain limitations. The assessment of changes in the tumor immune microenvironment after treatment was insufficient due to the lack of

antibody reagents for rabbits, which is the most suitable model for investigating TACE. Furthermore, the underlying mechanisms of the effects of combination therapy need to be further investigated.

The current study demonstrated that the combination of TACE and the LDHA inhibitor, Ox, resulted in a stronger antitumor immune response than that of the control, TACE and Ox groups inhibited angiogenesis and promoted increased survival in a rabbit VX2 liver tumor model. These findings indicated that targeting metabolic reprogramming could promote the efficacy of TACE, thus providing novel insights into the future application of a new treatment strategy in clinical practice for patients with advanced HCC.

Acknowledgements

Not applicable.

Funding

No funding was received.

Availability of data and materials

The datasets used and/or analyzed during the current study are available from the corresponding author on reasonable request.

Authors' contributions

JZ designed the research. YL and MY performed the experiments. YL and YY analyzed the data. JZ and YL wrote the paper. YL and JZ confirm the authenticity of all the raw data. All the authors read and approved the final manuscript.

Ethics approval and consent to participate

All animal studies were approved by the Animal Care and Use Committee of Huazhong University of Science and Technology (Wuhan, China; approval no. 3380) and were conducted in accordance with the institutional guidelines.

Patient consent for publication

Not applicable.

Competing interests

The authors declare that they have no competing interests.

References

1. Bray F, Ferlay J, Soerjomataram I, Siegel RL, Torre LA and Jemal A: Global cancer statistics 2018: GLOBOCAN estimates of incidence and mortality worldwide for 36 cancers in 185 countries. CA Cancer J Clin 68: 394-424, 2018.
2. Global Burden of Disease Cancer Collaboration; Fitzmaurice C, Allen C, Barber RM, Barregard L, Bhutta ZA, Brenner H, Dicker DJ, Chimed-Orchir O, Dandona R, *et al*: Global, regional, and national cancer incidence, mortality, years of life lost, years lived with disability, and disability-adjusted life-years for 32 cancer groups, 1990 to 2015: A systematic analysis for the global burden of disease study. JAMA Oncol 3: 524-548, 2017.
3. Arnold M, Abnet CC, Neale RE, Vignat J, Giovannucci EL, McGlynn KA and Bray F: Global burden of 5 major types of gastrointestinal cancer. Gastroenterology 159: 335-349.e15, 2020.
4. Sieghart W, Hucke F and Peck-Radosavljevic M: Transarterial chemoembolization: Modalities, indication, and patient selection. J Hepatol 62: 1187-1195, 2015.
5. Forner A, Gilabert M, Bruix J and Raoul JL: Treatment of intermediate-stage hepatocellular carcinoma. Nat Rev Clin Oncol 11: 525-535, 2014.
6. Sun B, Zhang L, Sun T, Ren Y, Cao Y, Zhang W, Zhu L, Guo Y, Gui Y, Liu F, *et al*: Safety and efficacy of lenvatinib combined with camrelizumab plus transcatheter arterial chemoembolization for unresectable hepatocellular carcinoma: A two-center retrospective study. Front Oncol 12: 982948, 2022.
7. Kroemer G and Pouyssegur J: Tumor cell metabolism: Cancer's Achilles' heel. Cancer Cell 13: 472-482, 2008.
8. Warburg O: On the origin of cancer cells. Science 123: 309-314, 1956.
9. Zheng J: Energy metabolism of cancer: Glycolysis versus oxidative phosphorylation (review). Oncol Lett 4: 1151-1157, 2012.
10. Robey IF, Stephen RM, Brown KS, Baggett BK, Gatenby RA and Gillies RJ: Regulation of the Warburg effect in early-passage breast cancer cells. Neoplasia 10: 745-756, 2008.
11. Iansante V, Choy PM, Fung SW, Liu Y, Chai JG, Dyson J, Del Rio A, D'Santos C, Williams R, Chokshi S, *et al*: PARP14 promotes the Warburg effect in hepatocellular carcinoma by inhibiting JNK1-dependent PKM2 phosphorylation and activation. Nat Commun 6: 7882, 2015.
12. Miao P, Sheng S, Sun X, Liu J and Huang G: Lactate dehydrogenase A in cancer: A promising target for diagnosis and therapy. IUBMB Life 65: 904-910, 2013.
13. Martinez-Outschoorn UE, Peiris-Pagés M, Pestell RG, Sotgia F and Lisanti MP: Cancer metabolism: A therapeutic perspective. Nat Rev Clin Oncol 14: 11-31, 2017.
14. Lee GH, Yan C, Shin SJ, Hong SC, Ahn T, Moon A, Park SJ, Lee YC, Yoo WH, Kim HT, *et al*: BAX inhibitor-1 enhances cancer metastasis by altering glucose metabolism and activating the sodium-hydrogen exchanger: The alteration of mitochondrial function. Oncogene 29: 2130-2141, 2010.
15. Gottfried E, Kunz-Schughart LA, Ebner S, Mueller-Klieser W, Hoves S, Andreesen R, Mackensen A and Kreutz M: Tumor-derived lactic acid modulates dendritic cell activation and antigen expression. Blood 107: 2013-2021, 2006.
16. Brand A, Singer K, Koehl GE, Kolitzus M, Schoenhammer G, Thiel A, Matos C, Bruss C, Klobuch S, Peter K, *et al*: LDHA-associated lactic acid production blunts tumor immunosurveillance by T and NK cells. Cell Metab 24: 657-671, 2016.
17. Le A, Cooper CR, Gouw AM, Dinavahi R, Maitra A, Deck LM, Royer RE, Vander Jagt DL, Semenza GL and Dang CV: Inhibition of lactate dehydrogenase A induces oxidative stress and inhibits tumor progression. Proc Natl Acad Sci USA 107: 2037-2042, 2010.
18. Huynh KN, Rao S, Roth B, Bryan T, Fernando DM, Dayyani F, Imagawa D and Abi-Jaoudeh N: Targeting hypoxia-inducible factor-1α for the management of hepatocellular carcinoma. Cancers (Basel) 15: 2738, 2023.
19. Goldman RD, Kaplan NO and Hall TC: Lactic dehydrogenase in human neoplastic tissues. Cancer Res 24: 389-399, 1964.
20. Zhai X, Yang Y, Wan J, Zhu R and Wu Y: Inhibition of LDH-A by oxamate induces G2/M arrest, apoptosis and increases radiosensitivity in nasopharyngeal carcinoma cells. Oncol Rep 30: 2983-2991, 2013.
21. Beckner ME, Stracke ML, Liotta LA and Schiffmann E: Glycolysis as primary energy source in tumor cell chemotaxis. J Natl Cancer Inst 82: 1836-1840, 1990.
22. Cassim S, Raymond VA, Dehbidi-Assadzadeh L, Lapierre P and Bilodeau M: Metabolic reprogramming enables hepatocarcinoma cells to efficiently adapt and survive to a nutrient-restricted microenvironment. Cell Cycle 17: 903-916, 2018.
23. Liu H, Savaraj N, Priebe W and Lampidis TJ: Hypoxia increases tumor cell sensitivity to glycolytic inhibitors: a strategy for solid tumor therapy (model C). Biochem Pharmacol 64: 1745-1751, 2002.
24. Qian K, Ma Y, Wan J, Geng S, Li H, Fu Q, Peng X, Kan X, Zhou G, Liu W, *et al*: The studies about doxorubicin-loaded p(N-isopropyl-acrylamide-co-butyl methylacrylate) temperature-sensitive nanogel dispersions on the application in TACE therapies for rabbit VX2 liver tumor. J Control Release 212: 41-49, 2015.

25. Liu Y, Shi D, Ren Y, Li L, Zhao Y, Zheng C and Yang X: The immune-chemo-embolization effect of temperature sensitive gold nanomedicines against liver cancer. Nano Res 16: 2749-2761, 2023.
26. Li X, Yu H, Huang Y, Chen Y, Wang J, Xu L, Zhang F, Zhuge Y and Zou X: Preparation of microspheres encapsulating sorafenib and catalase and their application in rabbit VX2 liver tumor. Biomed Pharmacother 129: 110512, 2020.
27. Masoud GN and Li W: HIF-1α pathway: Role, regulation and intervention for cancer therapy. Acta Pharm Sin B 5: 378-389, 2015.
28. Pouysségur J, Dayan F and Mazure NM: Hypoxia signalling in cancer and approaches to enforce tumour regression. Nature 441: 437-443, 2006.
29. Swietach P, Vaughan-Jones RD and Harris AL: Regulation of tumor pH and the role of carbonic anhydrase 9. Cancer Metastasis Rev 26: 299-310, 2007.
30. Gatenby RA and Gillies RJ: Why do cancers have high aerobic glycolysis? Nat Rev Cancer 4: 891-899, 2004.
31. Patra KC and Hay N: The pentose phosphate pathway and cancer. Trends Biochem Sci 39: 347-354, 2014.
32. Hermans D, Gautam S, García-Cañaveras JC, Gromer D, Mitra S, Spolski R, Li P, Christensen S, Nguyen R, Lin JX, *et al*: Lactate dehydrogenase inhibition synergizes with IL-21 to promote CD8+ T cell stemness and antitumor immunity. Proc Natl Acad Sci USA 117: 6047-6055, 2020.
33. Zhang YX, Zhao YY, Shen J, Sun X, Liu Y, Liu H, Wang Y and Wang J: Nanoenabled modulation of acidic tumor microenvironment reverses anergy of infiltrating T cells and potentiates anti-PD-1 therapy. Nano Lett 19: 2774-2783, 2019.
34. Daneshmandi S, Wegiel B and Seth P: Blockade of lactate dehydrogenase-A (LDH-A) improves efficacy of anti-programmed cell death-1 (PD-1) therapy in melanoma. Cancers (Basel) 11: 450, 2019.
35. Colegio OR, Chu NQ, Szabo AL, Chu T, Rhebergen AM, Jairam V, Cyrus N, Brokowski CE, Eisenbarth SC, Phillips GM, *et al*: Functional polarization of tumour-associated macrophages by tumour-derived lactic acid. Nature 513: 559-563, 2014.
36. Huang AC, Postow MA, Orlowski RJ, Mick R, Bengsch B, Manne S, Xu W, Harmon S, Giles JR, Wenz B, *et al*: T-cell invigoration to tumour burden ratio associated with anti-PD-1 response. Nature 545: 60-65, 2017.
37. Huang H: Matrix metalloproteinase-9 (MMP-9) as a cancer biomarker and MMP-9 biosensors: Recent advances. Sensors (Basel) 18: 3249, 2018.
38. Mondal S, Adhikari N, Banerjee S, Amin SA and Jha T: Matrix metalloproteinase-9 (MMP-9) and its inhibitors in cancer: A minireview. Eur J Med Chem 194: 112260, 2020.
39. Owyong M, Chou J, van den Bijgaart RJ, Kong N, Efe G, Maynard C, Talmi-Frank D, Solomonov I, Koopman C, Hadler-Olsen E, *et al*: MMP9 modulates the metastatic cascade and immune landscape for breast cancer anti-metastatic therapy. Life Sci Alliance 2: e201800226, 2019.
40. Nass RD, Wagner M, Surges R and Holdenrieder S: Time courses of HMGB1 and other inflammatory markers after generalized convulsive seizures. Epilepsy Res 162: 106301, 2020.
41. Apte RS, Chen DS and Ferrara N: VEGF in signaling and disease: Beyond discovery and development. Cell 176: 1248-1264, 2019.
42. Morse MA, Sun W, Kim R, He AR, Abada PB, Mynderse M and Finn RS: The role of angiogenesis in hepatocellular carcinoma. Clin Cancer Res 25: 912-920, 2019.
43. Raoul JL, Forner A, Bolondi L, Cheung TT, Kloeckner R and de Baere T: Updated use of TACE for hepatocellular carcinoma treatment: How and when to use it based on clinical evidence. Cancer Treat Rev 72: 28-36, 2019.